This manuscript differs from the one published in the ACM Digital Library in that the following corrections have been made:

- On page 3, the decomposition of step vectors originally attributed to Rechenberg [17] cannot be found in that reference. It is now attributed to Beyer [4]. As a result, the numbering of the references has changed.

- On page 4, integration bounds and an inequality have been corrected in the paragraphs containing Eqs. (5) and (6).

A Surrogate Model Assisted (1+1)-ES with Increased Exploitation of the Model

Jingyun Yang
Faculty of Computer Science
Dalhousie University
Halifax, Nova Scotia, Canada
Jingyun.Yang@dal.ca

Dirk V. Arnold
Faculty of Computer Science
Dalhousie University
Halifax, Nova Scotia, Canada
dirk@cs.dal.ca

ABSTRACT

Surrogate models in black-box optimization can be exploited to different degrees. At one end of the spectrum, they can be used to provide inexpensive but inaccurate assessments of the quality of candidate solutions generated by the black-box optimization algorithm. At the other end, optimization of the surrogate model function can be used in the process of generating those candidate solutions themselves. The latter approach more fully exploits the model, but may be more susceptible to systematic model error. This paper examines the effect of the degree of exploitation of the surrogate model in the context of a simple $(1 + 1)$-ES. First, we analytically derive the potential gain from more fully exploiting surrogate models by using a spherically symmetric test function and a simple model for the error resulting from the use of surrogate models. We then observe the effects of increased exploitation in an evolution strategy employing Gaussian process surrogate models applied to a range of test problems. We find that the gain resulting from more fully exploiting surrogate models can be considerable.

CCS CONCEPTS

• **Mathematics of computing → Bio-inspired optimization**; • **Computing methodologies → Continuous space search**;

KEYWORDS

Stochastic black-box optimization; evolution strategy; surrogate modelling

1 INTRODUCTION

Surrogate modelling techniques are commonly used when solving black-box optimization problems where the evaluation of the objective function is expensive. Models are built based on information gained through evaluation of the objective function in previous iterations. These models can then be used as inaccurate but inexpensive surrogates for the true objective function. Jin [8] and Loshchilov [13] provide surveys covering the use of surrogate modelling techniques in evolutionary computation.

Black-box optimization algorithms that employ surrogate models need to weigh the savings in cost from using those models against the potentially poor steps made as a result of their inaccuracy. Surrogate model assisted algorithms differ in the degree to which they exploit those models. One approach is to leave the generation of candidate solutions under the control of the black-box optimization algorithm. The surrogate model is used in place of the true objective function in order to avoid the costly evaluation of likely poor candidate solutions. An example of an algorithm that implements this approach is the Local Meta-Model Covariance Matrix Adaptation Evolution Strategy (lmm-CMA-ES) by Kern et al. [10]. A second approach is to involve the surrogate model in the generation of candidate solutions themselves. The surrogate model function is optimized in each iteration, and the optimizer of the surrogate model is subsequently evaluated using the true objective function. This approach is employed for example in the Gaussian Process Optimization Procedure (GPOP) by Büche et al. [6], who define several merit functions based on Gaussian process surrogate models in an attempt to balance exploitation and exploration. Arguably, the latter approach more fully exploits the surrogate models. At the same time, at least in its pure form, it may be more prone to make poor steps due to surrogate model error. Loshchilov et al. [15] explicitly address the degree of exploitation of surrogate models and empirically find that more intensive exploitation has the potential to provide a significant speed-up in their surrogate model assisted evolution strategy.

Implications of design decisions when incorporating surrogate models in black box optimization algorithms are not well understood. As a step toward understanding the consequences of different degrees of exploitation of surrogate models, we consider the performance of a surrogate model assisted $(1 + 1)$-ES[1]. The $(1 + 1)$-ES provides a baseline that has been well established since the early work of Rechenberg [17], and a large body of research concerning the performance of other evolution strategies relative to that of the $(1 + 1)$-ES exists [5]. Kayhani and Arnold [9] have studied the performance of a surrogate model assisted $(1 + 1)$-ES that minimally exploits the models in that they are used only to determine whether a candidate solution is to be evaluated by the objective function. They both analytically consider the performance of the algorithm on spherically symmetric test functions by using a simple model for

---

[1]See Hansen et al. [7] for evolution strategy terminology.

the error resulting from the use of surrogate models, and they experimentally evaluate it on a wider range of test functions. We use their algorithm, but generalize the approach to the generation of candidate solutions to potentially more intensively exploit surrogate models. Using their error model, we compare the speed-up resulting from more intensive exploitation relative to that of the strategy that minimally exploits the models. We then experimentally consider a range of test functions and find that while the benefits predicted under the simple error model for spherically symmetric functions cannot be fully realized, the gain from increased exploitation of the surrogate model can nonetheless be considerable.

The remainder of this paper is organized as follows. In Section 2 we review related work and introduce a surrogate model assisted $(1 + 1)$-ES with $(\mu/\mu, \lambda)$-preselection. Section 3 studies the performance of that algorithm on spherically symmetric objective functions by assuming a simple model for the error resulting from the use of surrogate models. Section 4 employs Gaussian process surrogate models and applies the algorithm to a range of test functions. Section 5 concludes with a brief discussion and proposed future work.

2 BACKGROUND AND ALGORITHM

Many approaches that employ surrogate models in evolutionary algorithms have been proposed. Jin [8] and Loshchilov [13] provide comprehensive overviews. Much recent work has focused on surrogate model assisted variants of covariance matrix adaptation evolution strategies (CMA-ES); see for example Loshchilov et al. [15] and Bajer et al. [3]. Our goal here is to study the impact of the degree of exploitation of the surrogate model on the performance of evolution strategies, and is thus orthogonal to the use of covariance matrix adaptation.

The value of surrogate modelling approaches is usually quantified through the notion of speed-up, which is defined as the number of objective function evaluations required to solve a given optimization problem using some black box optimization algorithm that does not employ surrogate models, divided by the number of objective function evaluations required by the corresponding algorithm that does use surrogate models. That is, it is assumed that the cost of surrogate modelling is negligible compared to the cost of evaluating the objective function.

A straightforward use of surrogate models has been proposed by Kern et al. [10]. Their algorithm in each iteration generates $\lambda > 1$ candidate solutions, employs a surrogate model that is based on information gained in previous iterations to generate estimates of their relative fidelities, and then uses the true objective function to evaluate those candidate solutions that score best under the model. The ratio of candidate solutions evaluated using the objective function is adapted based on whether the true objective function values that are obtained are in conflict with the ranking of the candidate solutions according to the surrogate model. As in each iteration at least one candidate solution is evaluated using the true objective function, the maximum speed-up compared to the strategy that uses the objective function to evaluate all λ candidate solutions is λ, but will be lower if the accuracy of the surrogate models is poor. Kern et al. [10] report experimentally observed speed-ups by factors between two and eight on unimodal functions, including

Input:
- candidate solution $\mathbf{x} \in \mathbb{R}^n$
- step size parameter $\sigma \in \mathbb{R}_{>0}$
- a surrogate model

1: Generate step vector $\mathbf{z} \in \mathbb{R}^n$ and let $\mathbf{y} = \mathbf{x} + \sigma\mathbf{z}$.
2: Evaluate $\mathbf{y}$ using the surrogate model, yielding $f_\epsilon(\mathbf{y})$.
3: **if** $f_\epsilon(\mathbf{y}) \geq f(\mathbf{x})$ **then**
4:     Let $\sigma \leftarrow \sigma\,\mathrm{e}^{-c_1/D}$.
5: **else**
6:     Evaluate $\mathbf{y}$ using the objective function, yielding $f(\mathbf{y})$.
7:     Update the surrogate model.
8:     **if** $f(\mathbf{y}) \geq f(\mathbf{x})$ **then**
9:         Let $\sigma \leftarrow \sigma\,\mathrm{e}^{-c_2/D}$.
10:     **else**
11:         Let $\mathbf{x} \leftarrow \mathbf{y}$ and $\sigma \leftarrow \sigma\,\mathrm{e}^{c_3/D}$.
12:     **end if**
13: **end if**

Figure 1: Single iteration of the surrogate model assisted $(1+1)$-**ES.**

Schwefel's ellipsoid and Rosenbrock's function, where dimensions range from two to sixteen.

Notice that candidate solutions in the algorithm by Kern et al. [10] are generated by the evolution strategy, and are thus random and unbiased. An algorithm that more fully exploits surrogate models is the Gaussian Process Optimization Procedure by Büche et al. [6]. In that algorithm, candidate solutions are obtained by in each iteration attempting to determine optimal solutions to merit functions that are based on the surrogate model function. Those solutions are then evaluated using the true objective function. Büche et al. [6] report speed-ups by a factor between four and five compared to CMA-ES on quadratic sphere functions and on Schwefel's ellipsoid, and smaller speed-ups on Rosenbrock's function.

We argue that it is meaningful to determine speed-up values relative to a well established baseline, and that in the context of evolution strategies, the $(1 + 1)$-ES forms a natural baseline. A surrogate model assisted variant of the $(1 + 1)$-ES has been proposed by Kramer [12]. That algorithm uses a surrogate model to evaluate the offspring candidate solution. If the value obtained suggests that the candidate solution is superior to the parental candidate solution from t iterations prior, then the objective function is used to establish its true fitness. The 1/5th rule [17] is used for the adaptation of the step size.

Kayhani and Arnold [9] consider that same algorithm for $t = 0$, but with a novel form of step size adaptation derived from the implementation of the 1/5th rule due to Kern et al. [11]. Assuming that the task at hand is minimization of function $f : \mathbb{R}^n \to \mathbb{R}$, a single iteration of that algorithm is detailed in Fig. 1. Parental candidate solution $\mathbf{x} \in \mathbb{R}^n$ and step size parameter $\sigma \in \mathbb{R}_{>0}$, together with an archive of those candidate solutions that have been evaluated using the objective function and that are used to generate the surrogate models, form the state of the algorithm. Step vector $\mathbf{z} \in \mathbb{R}^n$ is generated by sampling from a multivariate Gaussian distribution with

zero mean and unit covariance. The resulting offspring candidate solution $\mathbf{y} = \mathbf{x} + \sigma \mathbf{z}$ is then evaluated using the surrogate model function $f_\epsilon(\cdot)$. If the value obtained suggests that the offspring is inferior to the parent, then the step size is reduced. Otherwise, the offspring candidate solution is evaluated using the objective function, and it replaces the parent if and only if it is superior. The step size is increased in that case, and it is reduced if the parent prevails. Parameter $D > 0$ controls the speed with which the step size parameter can be adapted. Values for the coefficients $c_1, c_2, c_3 > 0$ are derived from an analysis of the performance of the algorithm on spherically symmetric test functions, using a simple model for surrogate model error to be detailed in Section 3. Employing Gaussian process surrogate models, speed-ups between 1.6 and 3.5 relative to the $(1 + 1)$-ES without surrogate model assistance are observed on several unimodal test functions.

The algorithm considered in this paper is identical to that considered by Kayhani and Arnold [9], save for the generation of step vectors in Line 1 of Fig. 1. Rather than sampling $\mathbf{z}$ from a zero mean Gaussian distribution, we sample $\lambda \geq 1$ trial step vectors $\mathbf{z}_i \in \mathbb{R}^n$, $i = 1, 2, \ldots, \lambda$, from a Gaussian distribution with zero mean and unit covariance. We then compute fitness estimates $f_\epsilon(\mathbf{x} + \sigma \mathbf{z}_i)$ using the surrogate model. Finally, using $k; \lambda$ to refer to the index of the kth smallest of the λ values observed, we compute the average

$$\mathbf{z} = \frac{1}{\mu} \sum_{k=1}^{\mu} \mathbf{z}_{k;\lambda} \tag{1}$$

of the $\mu \geq 1$ seemingly best trial steps as the step to be used in Line 1 of the algorithm in Fig. 1. As this approach to computing step vectors amounts to the same process as the generation of a step in the $(\mu/\mu, \lambda)$-ES, we refer to the resulting algorithm as the surrogate model assisted $(1 + 1)$-ES with $(\mu/\mu, \lambda)$-preselection. Notice that the algorithm makes no more than one true objective function evaluation per iteration, independent of λ. The algorithm bears similarities to the model assisted steady-state evolution strategy by Ulmer et al. [19], but differs in several aspects, including the averaging of trial step vectors and its mechanism for step size adaptation. Also notice that the algorithm considered by Kayhani and Arnold [9] is included as the special case that $\mu = \lambda = 1$. Choosing larger values for λ more intensively exploits the surrogate model in that the model is used to evaluate a larger number of points per iteration. Letting $\lambda \to \infty$, $f_\epsilon(\mathbf{x} + \sigma \mathbf{z}_{1;\lambda})$ will converge almost surely to the optimum of the surrogate model function. Practically, due to the inaccuracy of the surrogate models, we expect the gain from increasing λ to level off, and values of $\mu > 1$ to be useful.

3 ANALYSIS

This section studies the performance of the algorithm presented in Section 2 by considering spherically symmetric test function $f : \mathbb{R}^n \to \mathbb{R}$ with $f(\mathbf{x}) = \mathbf{x}^T \mathbf{x}$, using the simple model for the surrogate model error proposed by Kayhani and Arnold [9]. It generalizes the analysis presented there by considering step vectors from distributions other than a Gaussian distribution. Specifically, we consider the case that the step in Line 1 of the algorithm in Fig. 1 is generated by $(\mu/\mu, \lambda)$-preselection.

As Kayhani and Arnold [9], in this section we assume that the surrogate model error (i.e., the difference $f(\mathbf{y}) - f_\epsilon(\mathbf{y})$ between

the true objective function value of a candidate solution and its estimated value according to the surrogate model) can be modelled by an independent Gaussian random variable with mean zero and variance σ_ϵ^2, and that this variance is the same for all candidate solutions generated within an iteration. The standard deviation σ_ϵ is a measure for the quality of the surrogate model in that more accurate models correspond to smaller values of σ_ϵ. We expect the quality of this simple model to deteriorate as λ increases as especially the assumption of the independence of samples is unrealistic for deterministic surrogate models.

As proposed by Beyer [4], step vector $\mathbf{z}$ can be decomposed into a component $\mathbf{z}_1$ in the direction of the negative of the gradient of the objective function at $\mathbf{x}$ and a component $\mathbf{z}_{2\ldots n}$ orthogonal to the gradient direction. Due to the assumptions made with regard to the surrogate model error, the distribution of both components can be obtained from earlier work on the performance of the $(\mu/\mu, \lambda)$-ES applied to noisy spherically symmetric functions [1, 2]. Component $\mathbf{z}_{2\ldots n}$ is of random direction in the $(n-1)$-dimensional subspace orthogonal to the gradient. Its squared length for large dimensions is governed by $\lim_{n\to\infty} \|\mathbf{z}_{2\ldots n}\|^2/n = 1/\mu$. The component $\mathbf{z}_1$ of step vector $\mathbf{z}$ in direction of the negative gradient has a signed length with a probability density that cannot generally be given in closed form. However, expressions for the cumulants of the distribution can be obtained, allowing to approximate the density by using the initial terms in a Gram-Charlier expansion (see [18])

$$p_1(z) = \frac{1}{\sqrt{2\pi\kappa_2}} \exp\left(-\frac{(z - \kappa_1)^2}{2\kappa_2}\right)$$
$$\left[1 + \frac{\gamma_1}{3!} \mathrm{He}_3\left(\frac{z - \kappa_1}{\sqrt{\kappa_2}}\right) + \ldots\right], \quad (2)$$

where κ_k denotes the kth cumulant, $\mathrm{He}_k(\cdot)$ is the kth Hermite polynomial, and $\gamma_1 = \kappa_3/\kappa_2^{3/2}$ is the skewness of the distribution. Expressions for the first three cumulants are derived in [1, 2] and reproduced in the appendix below.

We refer to $\delta(\mathbf{z}) = n(f(\mathbf{x}) - f(\mathbf{x} + \sigma\mathbf{z}))/(2R^2)$, where $R = \|\mathbf{x}\|$, as the normalized fitness advantage associated with step vector $\mathbf{z}$. Introducing normalized step size $\sigma^* = n\sigma/R$, if $\mathbf{z}$ is generated through $(\mu/\mu, \lambda)$-preselection it follows that

$$\delta(\mathbf{z}) = \frac{n}{2R^2} \left(\mathbf{x}^T\mathbf{x} - (\mathbf{x} + \sigma\mathbf{z})^T(\mathbf{x} + \sigma\mathbf{z})\right)$$
$$= \frac{n}{2R^2} \left(-2\sigma\mathbf{x}^T\mathbf{z} - \sigma^2\|\mathbf{z}\|^2\right)$$
$$\stackrel{n\to\infty}{=} \sigma^* z_1 - \frac{\sigma^{*2}}{2\mu}, \tag{3}$$

where $\stackrel{n\to\infty}{=}$ denotes convergence in distribution, $z_1 = -\mathbf{x}^T\mathbf{z}/R$ is the signed length of the component of the step in the negative gradient direction, and the presence of μ in the denominator signifies the presence of genetic repair [5]. Moreover, introducing $\sigma_\epsilon^* = n\sigma_\epsilon/(2R^2)$, the estimated normalized fitness advantage associated with $\mathbf{z}$ (i.e., the normalized fitness advantage estimated by using the surrogate model to evaluate $\mathbf{y} = \mathbf{x} + \sigma\mathbf{z}$) is $\delta_\epsilon(\mathbf{z}) = \delta(\mathbf{z}) + \sigma_\epsilon^* z_\epsilon$, where z_ϵ is a random variable with Gaussian distribution with zero mean and unit variance.

The algorithm in Fig. 1 evaluates $\mathbf{y} = \mathbf{x} + \sigma\mathbf{z}$ using the objective function if and only if the estimated fitness advantage associated
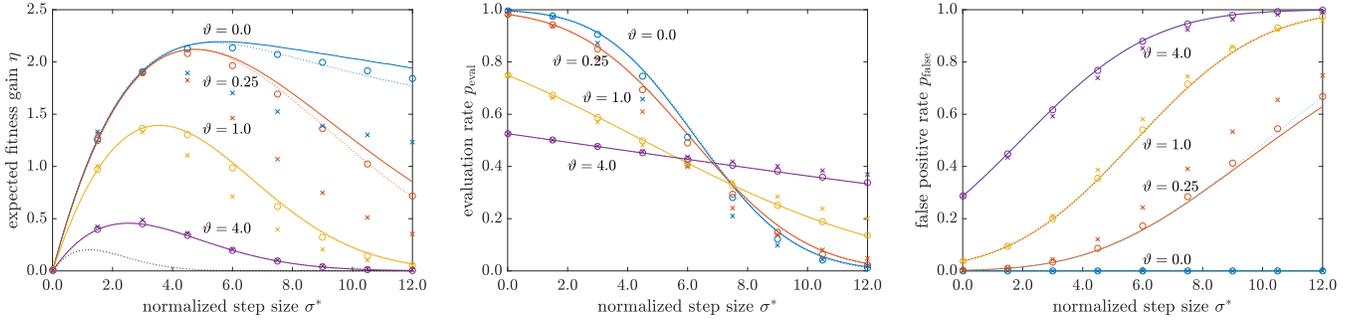
Figure 2: Expected single step behaviour of the surrogate model assisted $(1 + 1)$-ES with $(3/3, 10)$-preselection and unbiased Gaussian surrogate model error for noise-to-signal ratio $\vartheta \in \{0.0, 0.25, 1.0, 4.0\}$. The dashed and solid lines represent results obtained analytically in the limit $n \to \infty$ by considering Gram-Charlier approximations with cumulants up to the second and third included, respectively. The dots represent measurements made in runs of the algorithm with fixed normalized step size for $n = 100$ (circles) and $n = 10$ (crosses). The dotted black line in the leftmost subplot shows the expected fitness gain of the $(1 + 1)$-ES without surrogate model assistance.

with $\mathbf{z}$ is positive. The probability of using the objective function to evaluate a step generated using $(\mu/\mu, \lambda)$-preselection is thus

$$
\begin{aligned}
p_{\text{eval}} &= \text{Prob}\left[\delta_\epsilon(\mathbf{z}) > 0\right] \\
&= \frac{1}{\sqrt{2\pi}} \int_{-\infty}^{\infty} \int_{y_0(z)}^{\infty} e^{-\frac{1}{2}y^2} p_1(z) \, \mathrm{d}y \, \mathrm{d}z \\
&= \int_{-\infty}^{\infty} p_1(z) \, \Phi\left(\frac{\sigma^* z - \sigma^{*2}/(2\mu)}{\sigma_\epsilon^*}\right) \mathrm{d}z,
\end{aligned} \tag{4}
$$

where $\Phi(\cdot)$ is the cumulative distribution function of the Gaussian distribution with zero mean and unit variance, $p_1(\cdot)$ is the probability density function given in Eq. (2), and $y_0(z) = -(\sigma^* z - \sigma^{*2}/(2\mu))/\sigma_\epsilon^*$ is the value of z_ϵ below which δ_ϵ turns negative for given $z_1 = z$.

Similarly, the probability of using the objective function to evaluate a step generated by $(\mu/\mu, \lambda)$-preselection that has an associated negative fitness advantage is

$$
\begin{aligned}
p_{\text{false}} &= \text{Prob}\left[\delta(\mathbf{z}) < 0 \mid \delta_\epsilon(\mathbf{z}) > 0\right] \\
&= \frac{\text{Prob}[\delta(\mathbf{z}) < 0 \wedge \delta_\epsilon(\mathbf{z}) > 0]}{\text{Prob}[\delta_\epsilon(\mathbf{z}) > 0]} \\
&= \frac{1}{\sqrt{2\pi}p_{\text{eval}}} \int_{-\infty}^{\sigma^*/(2\mu)} \int_{y_0(z)}^{\infty} e^{-\frac{1}{2}y^2} p_1(z) \, \mathrm{d}y \, \mathrm{d}z \\
&= \frac{1}{p_{\text{eval}}} \int_{-\infty}^{\sigma^*/(2\mu)} p_1(z) \, \Phi\left(\frac{\sigma^* z - \sigma^{*2}/(2\mu)}{\sigma_\epsilon^*}\right) \mathrm{d}z
\end{aligned} \tag{5}
$$

as $\delta(\mathbf{z}) < 0$ is equivalent to $z_1 < \sigma^*/(2\mu)$. We refer to this probability as the false positive rate.

Finally, the expected value of the normalized change in objective function value

$$
\Delta = \begin{cases} \delta(\mathbf{z}) & \text{if } \delta_\epsilon(\mathbf{z}) > 0 \text{ and } \delta(\mathbf{z}) > 0 \\ 0 & \text{otherwise} \end{cases}
$$

from one iteration of the surrogate model assisted $(1 + 1)$-ES to the next can be computed as

$$
\begin{aligned}
\text{E}[\Delta] &= \frac{1}{\sqrt{2\pi}} \int_{\sigma^*/(2\mu)}^{\infty} \int_{y_0(z)}^{\infty} \left(\sigma^* z - \frac{\sigma^{*2}}{2\mu}\right) e^{-\frac{1}{2}y^2} p_1(z) \, \mathrm{d}y \, \mathrm{d}z \\
&= \int_{\sigma^*/(2\mu)}^{\infty} \left(\sigma^* z - \frac{\sigma^{*2}}{2\mu}\right) p_1(z) \, \Phi\left(\frac{\sigma^* z - \sigma^{*2}/2\mu}{\sigma_\epsilon^*}\right) \mathrm{d}z.
\end{aligned} \tag{6}
$$

With Eq. (2), Eqs. (4), (5), and (6) can be used to numerically compute the evaluation rate, the false positive rate, and the expected normalized change in objective function value of the strategy.

All of the equations thus derived consider only a single iteration of the surrogate model assisted $(1 + 1)$-ES. However, if a step size adaptation mechanism and surrogate modelling approach are in place such that the distributions of the normalized step size σ^* and the normalized surrogate model error strength σ_ϵ^* are invariant across iterations, then the algorithm converges linearly in expectation with dimension-normalized rate of convergence

$$
\begin{aligned}
c &= -\frac{n}{2} \text{E}\left[\log\left(\frac{f(\mathbf{x}_{t+1})}{f(\mathbf{x}_t)}\right)\right] \\
&= -\frac{n}{2} \text{E}\left[\log\left(1 - \frac{2\Delta}{n}\right)\right],
\end{aligned} \tag{7}
$$

where subscripts denote iteration number. As the rate of convergence does not account for computational cost and costs are incurred only in those iterations where a call to the objective function is made, we use $\eta = c/p_{\text{eval}}$ (normalized rate of convergence per objective function call) as performance measure and refer to it as the expected fitness gain. For $n \to \infty$ the logarithm in Eq. (7) can be linearized and the expected fitness gain is simply $\eta = \text{E}[\Delta]/p_{\text{eval}}$. We will see in experiments reported in Section 4 that linear convergence can indeed be achieved.

We define noise-to-signal ratio $\vartheta = \sigma_\epsilon^*/\sigma^*$ as a measure for the accuracy of the surrogate model relative to the step size of the algorithm. We run experiments with the surrogate model assisted $(1+1)$-ES as given in Fig. 1, but with Gaussian distributed surrogate model error in place of a true surrogate model and with the normalized step size set to a fixed value rather than being adapted. Figure 2
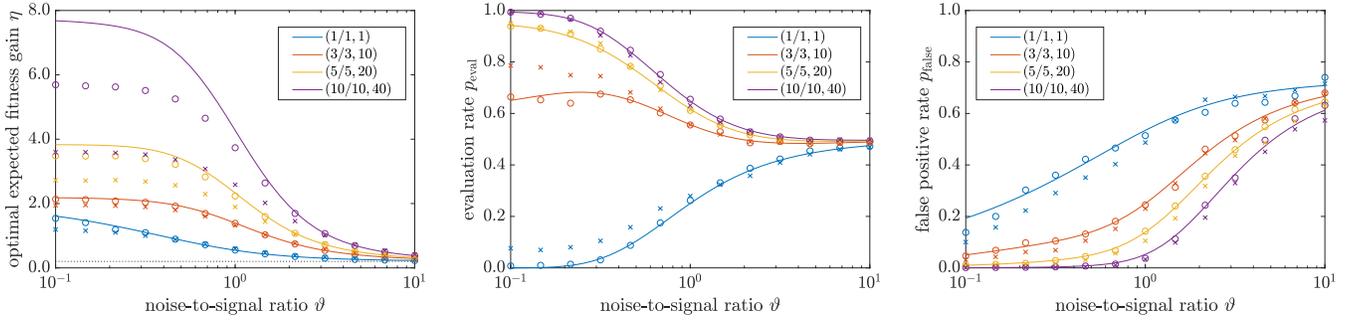
Figure 3: Single step performance of the surrogate model assisted $(1 + 1)$-ES with $(\mu/\mu, \lambda)$-preselection for optimally set normalized step size and unbiased Gaussian surrogate model error. The lines represent values obtained analytically in the limit $n \rightarrow \infty$, where cumulants up to the third have been considered. The dots represent experimental results for $n = 100$ (circles) and $n = 10$ (crosses). The dotted black line in the leftmost subplot shows the optimal expected fitness gain of the $(1 + 1)$-ES without surrogate model assistance.

plots the expected fitness gain η, the evaluation rate p_{eval}, and the false positive rate p_{false} against the normalized step size σ^*. The dots represent data measured in runs of the algorithm with $(3/3, 10)$-preselection in dimensions $n \in \{10, 100\}$ that have been averaged over 10^6 iterations. The dashed and solid lines represent analytically obtained results using cumulants up to the second (dashed lines) or third (solid lines). It can be seen that consideration of the skewness of the distribution has only a minor impact on the results. Deviations between experimental measurements and analytical predictions generally decrease with increasing dimension.

It can be seen from Fig. 2 that for given noise-to-signal ratio, the evaluation rate of the algorithm decreases with increasing normalized step size while the false positive rate increases. Unsurprisingly, false positive rates also increase with increasing noise-to-signal ratio. The expected fitness gain peaks at a finite value of the normalized step size and decreases with increasing noise-to-signal ratio. For $\vartheta \rightarrow \infty$ the surrogate model becomes useless and the expected fitness gain of the $(1 + 1)$-ES without surrogate model assistance (shown as a dotted black line in the plot) is recovered. As shown by Rechenberg [17], the optimal expected fitness gain of that strategy is 0.202 and achieved at a normalized step size of 1.224. The strategy with $(3/3, 10)$-preselection achieves expected fitness gain values significantly in excess of this, at larger normalized step sizes.

In order to illustrate the effect of increased exploitation of the surrogate model, Fig. 3 plots the optimal expected fitness gain (i.e., the fitness gain achieved for optimally set normalized step size) as well as the corresponding values of the evaluation rate and the false positive rate against the noise-to-signal ratio for $(\mu/\mu, \lambda)$-preselection with $\lambda \in \{1, 10, 20, 40\}$ and $\mu = \lceil \lambda/4 \rceil$. Notice that the results obtained for $\mu = \lambda = 1$ are the same as those obtained by Kayhani and Arnold [9]. It can be seen that the optimal expected fitness gain increases with increased exploitation of the model. With increasing noise-to-signal ratio, the curves approach the value of 0.202 attained without the use of surrogate models. As expected, in finite dimensions the gains predicted in the limit $n \rightarrow \infty$ cannot be fully realized, and for $n = 10$ the optimal expected fitness gain of the strategy with $(10/10, 40)$-preselection for small noise-to-signal ratios is only about half of the analytical prediction.

It is interesting to note that compared to the other strategy variants, the strategy with $(1/1, 1)$-preselection shows a fundamentally different relationship between noise-to-signal ratio and evaluation rate in Fig. 3. For the strategy with $\mu = \lambda = 1$, preselection is random and step vectors generated in Line 1 of the algorithm in Fig. 1 will form an obtuse angle with the gradient vector of the objective function as often as they form an acute one. What allows the strategy to outperform the $(1 + 1)$-ES without surrogate model assistance is its ability to operate with a significantly larger step size. The test in Line 3 of the algorithm in Fig. 1 serves as a filter, ensuring that for a majority of the generated (and mostly poor) steps no computational costs are incurred. In order to be maximally effective, the strategy needs to operate with an evaluation rate below 0.5. Strategies using $(\mu/\mu, \lambda)$-preselection with $\mu < \lambda$ on the other hand generate step vectors in Line 1 of the algorithm in Fig. 1 that predominantly have a positive component in the direction of the negative gradient. Optimal evaluation rates are much higher and increase with increasing exploitation of the surrogate model as the gains of the strategy are derived from the mostly beneficial steps, not from avoiding the evaluation of mostly poor ones. The rightmost subplot in Fig. 3 shows that this difference allows the strategy with $\mu < \lambda$ to operate with step sizes that afford significantly smaller false positive rates.

4 EXPERIMENTS

In order to further evaluate the proposed algorithm, we consider three families of test functions:

- Sphere functions $f(\mathbf{x}) = (\mathbf{x}^T\mathbf{x})^{\alpha/2}$ with $\alpha \in [0.25, 4.0]$. For $\alpha = 2$, this family includes the quadratic function considered in Section 3. The $(1 + 1)$-ES without surrogate model assistance achieves the same rate of convergence on all sphere functions. However, unless using comparison based surrogate models as proposed by Loshchilov et al. [14], surrogate models may exhibit different degrees of accuracy depending on α.
- Ellipsoid functions $f(\mathbf{x}) = \mathbf{x}^T\mathbf{A}\mathbf{x}$, where $n \times n$ matrix $\mathbf{A}$ equals $\text{diag}(\beta, 1, \ldots, 1)$ and $\beta \in [10^{-2}, 10^2]$. This family includes both

cigar ($\beta \ll 1$) and discus functions ($\beta \gg 1$). Parameter β controls the degree of ill-conditioning. For $\beta = 1$ the quadratic sphere function is recovered.

- Quartic functions $f(\mathbf{x}) = \sum_{i=1}^{n-1}[\gamma(x_{i+1} - x_i^2)^2 + (1 - x_i)^2]$, where $\mathbf{x} = (x_1, \ldots, x_n)^\mathrm{T}$, which combine the properties of being less than perfectly conditioned and being non-quadratic. For $\gamma = 100$, this family includes Rosenbrock's function, which is tedious to optimize without covariance matrix adaptation. We use $\gamma \in [1.0, 10.0]$. Ill-conditioning increases with increasing γ, with, depending on the dimension, condition numbers of the Hessian matrix at the optimizer between 33 and 50 for $\gamma = 1$, and numbers roughly 7.5 times higher for $\gamma = 10$.

All of the test problems are considered in dimensions $n \in \{2, 4, 8, 16\}$. Runs are initialized by sampling starting points $\mathbf{x}$ from a Gaussian distribution with mean zero and with coordinate-wise standard deviations of 1000 for the sphere and ellipsoid functions and 1 for the quartic functions. The step size parameter is initialized to $\sigma = 1000$ for the sphere and ellipsoid functions and to $\sigma = 1$ for the quartic functions. The optimal function value of all test problems is zero. As Rosenbrock's function, the quartic functions with $n \geq 4$ have a second local minimizer. The stopping criteria used are for the evolution strategy to evaluate a candidate solution with an objective function value below 10^{-12}, to evaluate a candidate solution within a radius of 10^{-8} of the global optimizer, or to decrease the step size parameter below 10^{-15}. The only runs in which the third termination criterion was triggered were those that converged to the second local minimizer of the quartic functions.

Two further things are needed in order to be able to test the surrogate model assisted $(1 + 1)$-ES: a "true" surrogate model to replace the assumption of Gaussian distributed surrogate model error, and suitable values for the parameters that control the adaptation of the step size in the algorithm in Fig. 1. For the former, we use Gaussian process models with a squared exponential kernel [16]. We train the surrogate models by using the $N = 8n$ most recently evaluated points as the training set and use the Gaussian process's mean prediction as an estimate of the true objective function value. By limiting the training set to a fixed number of points we avoid the issue of the computational cost of model fitting increasing with increasing number of iterations. We do not use surrogate models in the first N iterations of a run and revert to the simple $(1 + 1)$-ES with the 1/5th success rule instead. We set the length scale parameter of the squared exponential kernel to $8n\sigma$. The proportionality of the length scale parameter, which governs how rapidly correlations between objective function values decrease, to the step size parameter of the evolution strategy is motivated by the desire to achieve scale invariance and consequently linear convergence. The constant of proportionality has been obtained in preliminary experiments and for the problems considered yields results somewhat superior to those observed using the setting employed by Kayhani and Arnold [9]. Finally, we use values of $c_1 = 0.05$, $c_2 = 0.2$, and $c_3 = 0.6$ for the strategy with $(1/1, 1)$-preselection as proposed by Kayhani and Arnold [9]. When more fully exploiting the surrogate model and doing $(\mu/\mu, \lambda)$-preselection with $\lambda > \mu$, we use $c_1 = 0.2$ and $c_2 = c_3 = 1.0$ in order to account for the qualitatively different operating behaviour of the algorithm observed in Fig. 3. We use $D = \sqrt{n+1}$ in all cases.

For each test problem considered, we have conducted 101 runs of the $(1 + 1)$-ES without surrogate model assistance as well as of the surrogate model assisted algorithm using $(\mu/\mu, \lambda)$-preselection with $\lambda \in \{1, 10, 20, 40\}$ and $\mu = \lceil \lambda/4 \rceil$. Runs that converged to the second local minimizer of the quartic functions were repeated until convergence to the global optimizer was achieved. Figure 4 illustrates runs on several problem instances in detail; Fig. 5 summarizes all of the results.

The top row in Fig. 4 shows logarithmic histograms of the numbers of objective function evaluations required to reach termination accuracy. It can be seen that surrogate model assistance consistently results in substantial savings. The remaining rows of Fig. 4 illustrate those surrogate model assisted runs that required the median number of objective function evaluations to terminate. From the second row, it can be seen that all strategy variants appear to achieve linear convergence for all test problems shown, demonstrating that the adaptation of the step size is successful and that the local Gaussian process surrogate models allow the evolution strategy to operate under an eventually flat noise-to-signal ratio. This is further illustrated in the bottom row of Fig. 4, where the relative model error, defined as the absolute deviation of surrogate model estimates from true objective function values, divided by the absolute difference between objective function values of parent and offspring, appears to be characterized by a distribution that is stationary after initialization effects have faded.

Figure 5 shows speed-up values of the surrogate model assisted $(1 + 1)$-ES relative to the $(1 + 1)$-ES without surrogate model assistance, where speed-up is defined as the median number of objective function evaluations required to satisfy a termination criterion by the strategy without surrogate model assistance divided by the corresponding median number of objective function evaluations of the algorithm with surrogate model assistance. It can be seen that all speed-up values are in excess of 1.0, indicating that surrogate model assistance is beneficial throughout. It can also be seen that in almost all cases, preselection with $\lambda > \mu$ is superior to preselection with $\mu = \lambda = 1$ and that the benefits generally increase with increasing degree of exploitation of the surrogate model.

Speed-up values observed for sphere functions peak at $\alpha = 2$, where the Gaussian process surrogate models provide the highest accuracy. Speed-up values for $\alpha > 2$ decrease rather rapidly, indicating that Gaussian process models are less than well suited for those problems. Indeed, sphere functions with values of $\alpha > 2$ are the only test problems considered where median runs of the strategy with minimal exploitation of the surrogate model in some cases are superior to those of the strategy with more intensive exploitation. Speed-up values for $(1/1, 1)$-preselection and sphere functions with $\alpha \leq 2$ range from 2.5 to 6.1 for $n = 2$ and from 1.8 to 3.4 for $n = 16$. More intensive exploitation of the model through $(10/10, 40)$-preselection achieves significantly higher speed-up values between 3.9 and 7.0 for $n = 2$ and between 2.9 and 4.4 for $n = 16$.

For the ellipsoid functions, more intensive exploitation of the model results in significantly higher speed-ups for some of the less well conditioned problem instances. Speed-up values observed for the cigar function with $\beta = 0.01$ and $(10/10, 40)$-preselection can range as high as nearly 40.0, but except for the smallest dimensions decrease with increasing dimension. Increased surrogate model
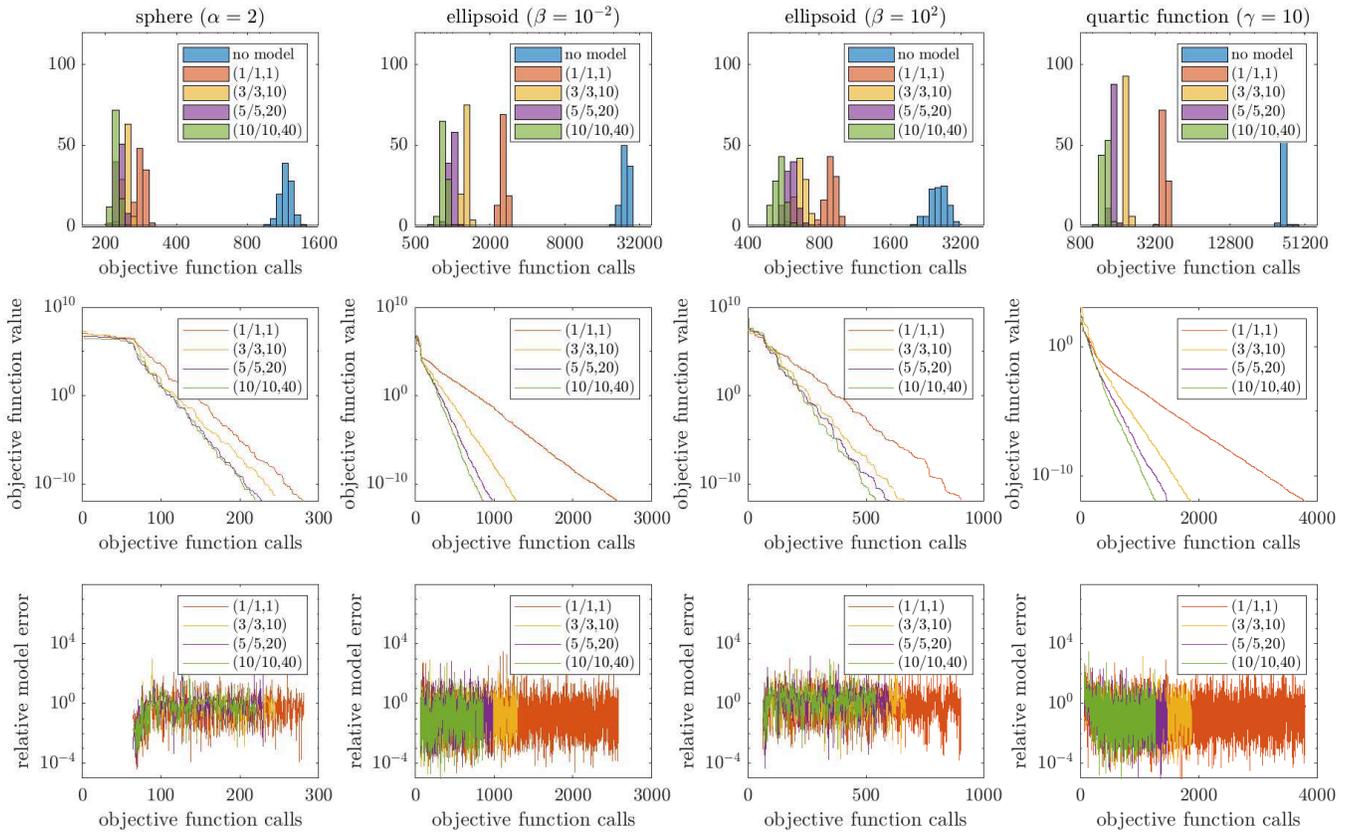
Figure 4: Histograms and median runs for selected test problems with $n = 8$. The columns from left to right show results for the quadratic sphere, cigar and discus with $\beta = 0.01$ and 100.0, respectively, and the quartic function with $\gamma = 10$. The top row shows logarithmic histograms of the number of objective function evaluations required to attain termination accuracy for the $(1 + 1)$-ES without surrogate model assistance as well for surrogate model assisted $(1 + 1)$-ES with $(\mu/\mu, \lambda)$-preselection for $\lambda \in \{1, 10, 20, 40\}$ and $\mu = \lceil \lambda/4 \rceil$. The second and third rows show objective function values and relative model error observed in the median runs of the surrogate model assisted algorithms.

exploitation in some instances triples the speed-up achieved by the surrogate model assisted strategy with $(1/1, 1)$-preselection. Speed-up values observed for the discus functions with $\beta = 100$ are lower except in low dimensions, suggesting that either the Gaussian process surrogate models do not adequately model a narrow one-dimensional valley if the dimension exceeds $n = 8$ or that step size adaption works less than well.

For the quartic test problems, speed-up values observed generally increase with increasing degree of ill-conditioning, and they decrease with increasing dimension. While more intensive exploitation of the surrogate model provides only small benefits for $n = 2$, $(10/10, 40)$-preselection achieves roughly between two and three times the speed-up of $(1/1, 1)$-preselection for $n \in \{8, 16\}$.

5 CONCLUSIONS

To conclude, we have proposed a surrogate model assisted $(1+1)$-ES with variable exploitation of the model. Compared with the surrogate model assisted $(1+1)$-ES by Kayhani and Arnold [9], evaluating multiple trial steps using the surrogate model before considering a

step to be evaluated by the objective function allows the strategy to likely consider better steps. An analysis of the algorithm applied to spherically symmetric test functions using a very simple model for the surrogate model error suggests that the performance gains resulting from preselection with $\lambda > \mu$ result from a fundamentally different source than those observed by Kayhani and Arnold [9]. Rather than relying on large steps and a low evaluation rate, it is the more beneficial steps resulting from preselection that allow the algorithm to succeed. An experimental comparison using Gaussian process surrogate models and considering several families of test functions suggests that the benefits from $(\mu/\mu, \lambda)$-preselection with $\lambda > \mu$ can indeed be substantial. Moreover, for most of the test problems, λ has been observed to be an uncritical parameter in that increasing its value (at least within the range of values considered here) does not negatively affect the strategy's performance.

In future work we plan to implement covariance matrix adaptation in the surrogate model assisted $(1 + 1)$-ES in order to see whether the observed benefits on less than perfectly well conditioned problems observed here persist when ill-conditioning is
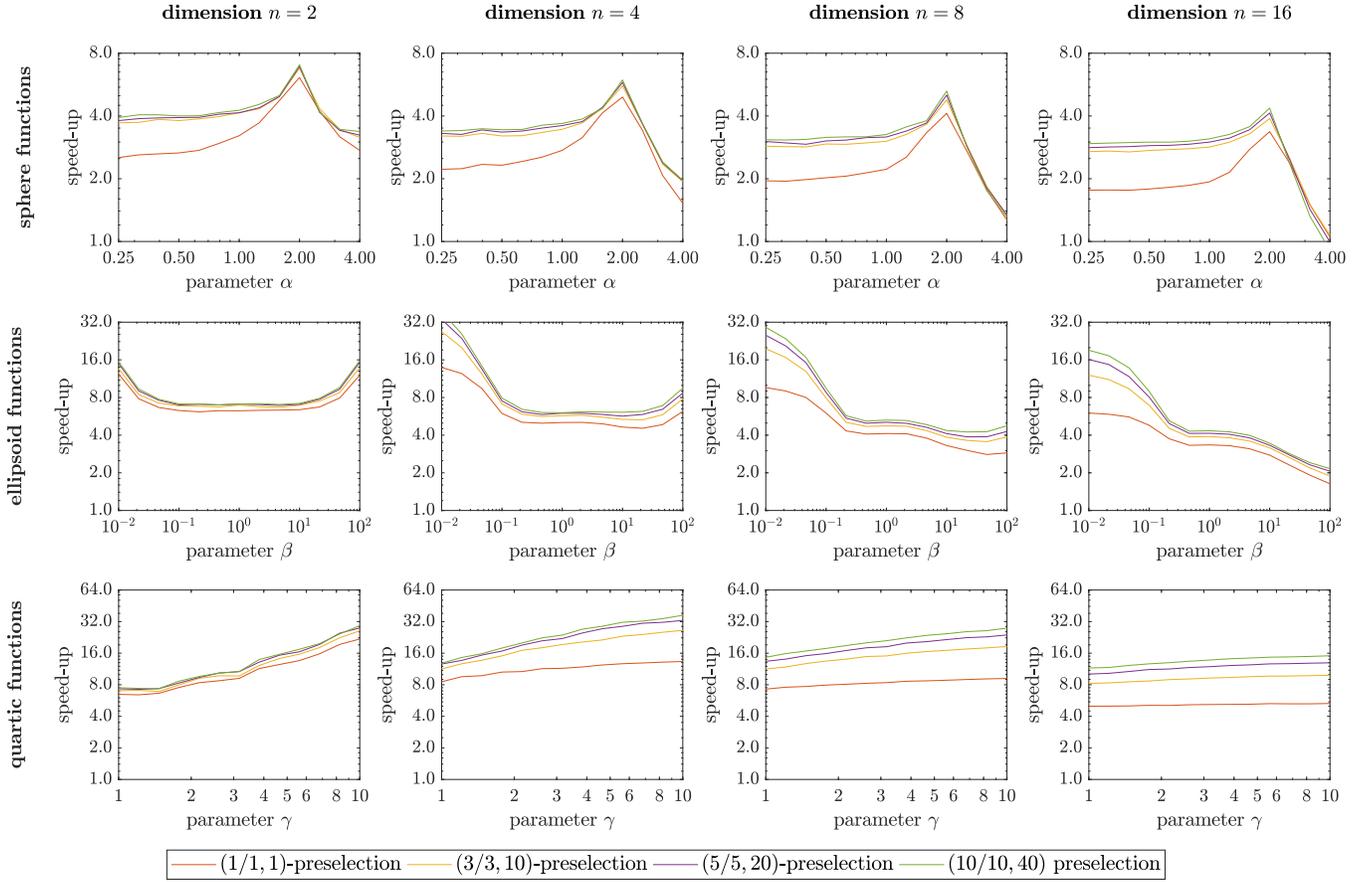
Figure 5: Speed-ups observed in median runs. From top to bottom, the rows show results for sphere functions, ellipsoid functions, and quartic functions. The columns hold results for dimensions for, from left to right, $n = 2$, 4, 8, and 16. The plots show the speed-ups of surrogate model assisted (1+1)-ES with $(\mu/\mu, \lambda)$-preselection for $\lambda \in \{1, 10, 20, 40\}$ and $\mu = \lceil \lambda/4 \rceil$.

addressed by the evolution strategy itself. Considering covariance matrix adaptation will also allow comparing the performance of the surrogate model assisted $(1 + 1)$-ES with $(\mu/\mu, \lambda)$-preselection with that of other surrogate model assisted black box optimization algorithms that employ covariance matrix adaptation and thus other approaches to the exploitation of surrogate models. Finally, we will consider strategies for adapting the parameters of the Gaussian process surrogate models, including the size of the training set and the length scale parameter.

ACKNOWLEDGEMENTS

A APPENDIX

Cumulants of the distribution of the signed length of the component of the step vector in the direction of the negative gradient of the objective function resulting from $(\mu/\mu, \lambda)$-preselection can be obtained by computing expectations of concomitants of order statistics of the Gaussian distribution. Arnold and Beyer [1, 2] derive

the following expressions for the first three cumulants:

$$
\kappa_1 = a h_{\mu,\lambda}^{1,0}
$$
$$
\kappa_2 = \frac{1}{\mu}\left(1 + a^2 h_{\mu,\lambda}^{1,1}\right) + \frac{\mu - 1}{\mu} a^2 h_{\mu,\lambda}^{2,0} - \kappa_1^2
$$
$$
\kappa_3 = \frac{1}{\mu^2}\left(3 h_{\mu,\lambda}^{1,0} + a^2 h_{\mu,\lambda}^{1,2}\right) + 3\frac{\mu - 1}{\mu^2} a \left(h_{\mu,\lambda}^{1,0} + a^2 h_{\mu,\lambda}^{2,1}\right)
$$
$$
+ \frac{(\mu - 1)(\mu - 2)}{\mu^2} a^3 h_{\mu,\lambda}^{3,0} - \frac{3}{\mu}\kappa_1\left(1 + a^2 h_{\mu,\lambda}^{1,1}\right)
$$
$$
- 3\frac{\mu - 1}{\mu}\kappa_1 a^2 h_{\mu,\lambda}^{2,0} + 2\kappa_1^3
$$

where $a = 1/\sqrt{1 + \vartheta^2}$ with noise-to-signal ratio ϑ as defined in Section 3, and

$$
h_{\mu,\lambda}^{i,k} = \frac{\lambda - \mu}{\sqrt{2\pi}}\binom{\lambda}{\mu}\int_{-\infty}^{\infty} \mathrm{He}_k(x)\mathrm{e}^{-\frac{1}{2}x^2}
$$
$$
[\phi(x)]^i[\Phi(x)]^{\lambda - \mu - 1}[1 - \Phi(x)]^{\mu - i}\mathrm{d}x
$$

with $\phi(\cdot)$ and $\Phi(\cdot)$ being the probability density and cumulative distribution functions of the standard Gaussian distribution.

REFERENCES

[1] D. V. Arnold. 2002. *Noisy Optimization with Evolution Strategies*. Kluwer Academic Publishers.

[2] D. V. Arnold and H.-G. Beyer. 2005. Expected sample moments of concomitants of selected order statistics. *Statistics and Computing* 15, 3 (2005), 241–250.

[3] L. Bajer, Z. Pitra, J. Repický, and M. Holeňa. 2019. Gaussian process surrogate models for the CMA evolution strategy. *Evolutionary Computation* (2019). to appear.

[4] H.-G. Beyer. 1993. Toward a theory of evolution strategies: Some asymptotical results from the $(1 \overset{+}{,} \lambda)$-theory. *Evolutionary Computation* 1, 2 (1993), 165–188.

[5] H.-G. Beyer. 2001. *The Theory of Evolution Strategies*. Springer Verlag.

[6] D. Büche, N. N. Schraudolph, and P. Koumoutsakos. 2005. Accelerating evolutionary algorithms with Gaussian process fitness function models. *IEEE Transactions on Systems, Man, and Cybernetics, Part C* 35, 2 (2005), 183–194.

[7] N. Hansen, D. V. Arnold, and A. Auger. 2015. Evolution strategies. In *Springer Handbook of Computational Intelligence*, J. Kacprzyk and W. Pedrycz (Eds.). Springer Verlag, 871–898.

[8] Y. Jin. 2011. Surrogate-assisted evolutionary computation: Recent advances and future challenges. *Swarm and Evolutionary Computation* 1, 2 (2011), 61–70.

[9] A. Kayhani and D. V. Arnold. 2018. Design of a surrogate model assisted $(1 + 1)$-ES. In *Parallel Problem Solving from Nature — PPSN XV*, A. Auger et al. (Eds.). Springer Verlag, 16–28.

[10] S. Kern, N. Hansen, and P. Koumoutsakos. 2006. Local meta-models for optimization using evolution strategies. In *Parallel Problem Solving from Nature — PPSN IX*, T. P. Runarsson et al. (Eds.). Springer Verlag, 939–948.

[11] S. Kern, S. D. Müller, N. Hansen, D. Büche, J. Ocenasek, and P. Koumoutsakos. 2004. Learning probability distributions in continuous evolutionary algorithms — A comparative review. *Natural Computing* 3, 1 (2004), 77–112.

[12] O. Kramer. 2016. *Machine Learning for Evolution Strategies*. Springer Verlag.

[13] I. Loshchilov. 2013. *Surrogate-Assisted Evolutionary Algorithms*. Ph.D. Dissertation. Université Paris Sud – Paris XI.

[14] I. Loshchilov, M. Schoenauer, and M. Sebag. 2012. Comparison-based optimizers need comparison-based surrogates. In *Parallel Problem Solving from Nature — PPSN XI*, R. Schaefer et al. (Eds.). Springer Verlag, 364–373.

[15] I. Loshchilov, M. Schoenauer, and M. Sebag. 2013. Intensive surrogate model exploitation in self-adaptive surrogate-assisted CMA-ES. In *Genetic and Evolutionary Computation Conference — GECCO 2013*. ACM Press, 439–446.

[16] C. E. Rasmussen and C. K. I. Williams. 2006. *Gaussian Processes for Machine Learning*. MIT Press.

[17] I. Rechenberg. 1973. *Evolutionsstrategie — Optimierung technischer Systeme nach Prinzipien der biologischen Evolution*. Friedrich Frommann Verlag.

[18] A. Stuart and J. K. Ord. 1994. *Kendall's Advanced Theory of Statistics* (sixth ed.). Vol. I: Distribution Theory. Wiley.

[19] H. Ulmer, F. Streichert, and A. Zell. 2003. Model-assisted steady-state evolution strategies. In *Genetic and Evolutionary Computation Conference — GECCO 2003*, E. Cantú-Paz et al. (Eds.). Springer Verlag, 610–621.